Molecular engineering of a cobalt-based electrocatalytic nanomaterial for H₂ evolution under fully aqueous conditions

Eugen S. Andreiadis[1], Pierre-André Jacques[1], Phong D. Tran[1], Adeline Leyris[2],
Murielle Chavarot-Kerlidou[1], Bruno Jousselme[3], Muriel Matheron[2], Jacques Pécaut[4],
Serge Palacin[3], Marc Fontecave[1,5] and Vincent Artero[1]*

The viability of a hydrogen economy depends on the design of efficient catalytic systems based on earth-abundant elements. Innovative breakthroughs for hydrogen evolution based on molecular tetraimine cobalt compounds have appeared in the past decade. Here we show that such a diimine–dioxime cobalt catalyst can be grafted to the surface of a carbon nanotube electrode. The resulting electrocatalytic cathode material mediates H₂ generation (55,000 turnovers in seven hours) from fully aqueous solutions at low-to-medium overpotentials. This material is remarkably stable, which allows extensive cycling with preservation of the grafted molecular complex, as shown by electrochemical studies, X-ray photoelectron spectroscopy and scanning electron microscopy. This clearly indicates that grafting provides an increased stability to these cobalt catalysts, and suggests the possible application of these materials in the development of technological devices.

In the context of the increasing global energy demand and continuous depletion of fossil fuel-reserves, the exploitation of renewable carbon-neutral energy sources, such as sunlight, is one of the greatest scientific challenges of this century[1]. As their availability does not strictly meet the demand, energy from renewable sources must, however, be stored durably for further use. The production of hydrogen through water splitting, either electrochemically or photochemically, seems to be a promising and sustainable solution to the storage of energy in a chemical and stable form, before converting it back into electricity, for example in a hydrogen-driven fuel cell[2]. Electrocatalysis is the key enabling technology for these processes[3]. However, precious metals, namely platinum, are often used for H₂-related applications, although they are neither cheap nor sustainable resources[4]. There is thus a crucial need to design efficient systems based on earth-abundant first-row transition metals that are capable of producing H₂ from water with high catalytic activity and stability.

Innovative breakthroughs based on cobalt compounds have appeared during the recent decade[5,6] for both hydrogen-evolution and water-oxidation reactions[7–11]. We[12,13] and others[14,15] reported that a series of cobaloxime compounds displays remarkable properties for proton reduction in non-aqueous solvents with low overpotential requirements[16]. However, practical applications of such molecular catalysts require their incorporation in electrode materials that can operate with fully aqueous electrolytes, as previously demonstrated with DuBois' nickel-based system[17–19]. In these studies and others that involve water-oxidation catalysts[20–22], carbon nanotubes (CNTs) were chosen as electrode materials for the following reasons: first, they provide large surface areas and thus a high catalyst loading[23]; second, electrodes based on CNTs display remarkable properties in terms of stability and electronic conductivity[24,25]; third, versatile and straightforward methods[26], such as electroreduction of functionalized aryldiazonium salts[27], are available for grafting molecular complexes onto various carbon materials such as CNTs.

As a first step towards this goal, recently we reported[28] a second generation of cobalt H₂-evolving catalysts, based on a tetradentate diimine–dioxime ligand, that display excellent catalytic properties (in terms of overpotential requirement and turnover frequencies) combined with greater stabilities compared with those of the previously reported cobaloximes. Here we show that these second-generation catalysts can be used for the molecular engineering of a H₂-evolving cathode material working in a purely aqueous electrolyte at small-to-moderate overpotentials and mild pH. The retention of the catalytic activity on grafting also allows us to derive conclusions about the heterolytic nature of the H₂-evolving step, still under debate for this class of catalysts[5].

Results and discussion

Derivatization of the diimine–dioxime cobalt catalyst. Cobaloxime compounds can only be covalently functionalized at the substituent of the glyoxime ligand. Owing to the innate reactivity of these complexes, ligand modification must be achieved before assembly of the complex, which leads to undesired symmetrical polyfunctionalized complexes. By contrast, cobalt diimine–dioxime complexes are well suited for a selective monofunctionalization on the C3 hydrocarbon chain of the tetradentate diimine–dioxime ligand N_2,N_2-propanediylbis(2,3-butanedione 2-imine 3-oxime ((DOH)₂pn): an azido group can be introduced in a straightforward manner thanks to its inertness under the harsh conditions required for the bis-ketimine condensation. Moreover, azido groups react selectively with

[1]Laboratoire de Chimie et Biologie des Métaux (CEA/Université Grenoble 1/CNRS), 17 rue des Martyrs, F-38054 Grenoble Cedex 9, France, [2]Department of Technology for Biology and Health, CEA LETI-MINATEC, 17 rue des Martyrs, F-38054 Grenoble Cedex 9, France, [3]CEA, IRAMIS, SPCSI, Chemistry of Surfaces and Interfaces Group, F-91191 Gif sur Yvette Cedex, France, [4]CEA, INAC, LCIB (UMR-E 3 CEA, UJF-Grenoble 1), 17 rue des Martyrs, F-38054 Grenoble Cedex 9, France, [5]Collège de France, 11 place Marcelin-Berthelot, F-75231 Paris Cedex 5, France. *e-mail: vincent.artero@cea.fr

various alkyne-containing substrates via azide–alkyne cycloaddition (the most famous reaction in click chemistry)[29] under smooth conditions, usually compatible with most organic and metallorganic functions.

The azido-functionalized diimine–dioxime ligand **1** was prepared from commercially available 2-hydroxy-1,3-diaminopropane (**I**) in five steps (via N,N'-di-t-boc-2-azido-1,3-diaminopropane (**II**) (boc = butyloxycarbonyl) and 2-azido-1,3-diaminopropane hydrochloride salt (**III**) (the full synthetic protocol is given in the Supplementary Information). Reaction of **1** with Co(II) chloride in the presence of air led to the pure [Co(III)(DO)(DOH)N$_3$-pnCl$_2$] complex **2** in very good yield. The molecular structure of the complex was solved by X-ray crystal diffraction (Fig. 1) and shows an octahedral environment around the cobalt(III) ion with two axial chloride ligands located in *trans* positions.

Fabrication of CNT electrodes. Standard copper-catalysed conditions for the azide–alkyne cycloaddition reaction resulted in substitution of the cobalt ion by a copper one. We then used Bertozzi's copper-free click methodology based on a strained functionalized cyclooctyne[30] to attach the azido derivative **2** onto an electrode made of amino-functionalized multiwalled CNTs[18] (MWCNTs, Fig. 1). First, we prepared the N-hydroxy-phthalimide-activated ester **V** from 2-(cyclooct-2-yn-1-yloxy)ethanoic acid (**IV**) and clicked it with **2** to yield the cobalt(III) complex **3**, which was isolated and purified. Cyclic voltammograms in the presence of anilinium tetrafluoroborate in acetonitrile (Supplementary Fig. S1) and bulk electrolysis experiments showed that **3** is active for electrocatalytic H$_2$ evolution with an overpotential requirement of 185 mV, significantly lower than that of the non-substituted [Co(DO)(DOH)pnBr$_2$] complex (290 mV) (ref. 16). Using the catalytic current enhancement, expressed as the i_c/i_p ratio (i_c is the catalytic current and i_p the peak current associated with the Co(II/I) couple) as a proxy for the catalytic turnover frequency, we showed that **3** is a slower catalyst than **2** (Supplementary Fig. S2), as already observed for nickel catalysts[18]. Clearly, this indicates that flexibility at the propylene bridge promotes reorganisation around Co as it cycles through various oxidation states during hydrogen evolution.

In parallel, a mixture of Nafion and MWCNTs was deposited on a gas-diffusion layer (GDL) electrode. Then the MWCNTs were decorated with a poly-4-(2-aminoethyl)phenylene layer (schematically represented in Fig. 1) through the electroreduction of the corresponding aryldiazonium salt, as previously described[23]. Finally, cobalt complex **3** was attached covalently to the electrode under smooth conditions through amide linkages generated during the reaction (in CH$_2$Cl$_2$ at room temperature and in the presence of 2,6-lutidine) of the activated ester **3** with the grafted amine residues. A schematic representation of the resulting functionalized CNT–Co material is displayed in Fig. 1.

Characterization of the electrode material. Figure 2 shows the cyclic voltammogram recorded for the functionalized electrode. Comparison with that measured for bulk **3** at a similar, but unfunctionalized, GDL/MWCNT electrode in CH$_3$CN clearly indicates that the structure of the cobalt complex was retained on grafting. Both display a well-defined reversible process at -1.08 V versus ferrocenium/ferrocene (Fc$^+$/Fc), assigned to the Co(II)/Co(I) couple of the complex[31]. For the functionalized material, the reversibility of the Co(III)/Co(II) process, associated with chloride elimination from the Co(III) centre, could be resolved partially near -0.6 V versus Fc$^+$/Fc only if a concentrated chloride solution was used as the electrolyte. Only the Co(II)/Co(I) process was seen in the absence of chloride anions in solution (Supplementary Fig. S9). The intensities of
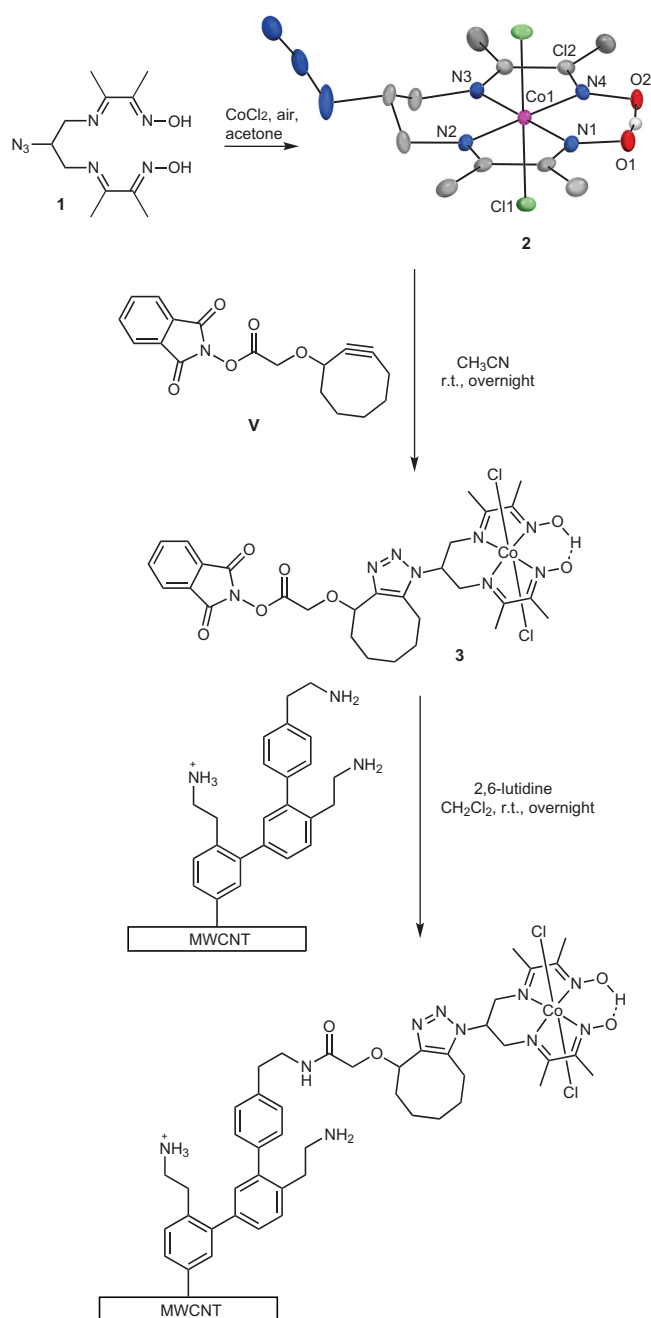

Figure 1 | Synthetic methodology for the preparation of the CNT/Co material. The number of phenylene residues in the structure of the amino-decorated MWCNTs is arbitrary. The X-ray structure of **2** is also shown (CCDC 896938, ORTEP diagram, 35% probability level displacement ellipsoids), with hydrogen atoms (except the bridging H in HO$_2$) omitted for clarity. Selected bond lengths (Å) and angles (°): Co(1)–N(1) = 1.8920(14), Co(1)–N(4) = 1.8970(13), Co(1)–N(3) = 1.9111(15), Co(1)–N(2) = 1.9162(14), Co(1)–Cl(1) = 2.2363(5), Co(1)–Cl(2) = 2.2436(5), N(1)–Co(1)–N(4) = 97.60(6), N(1)–Co(1)–N(3) = 179.10(7), N(4)–Co(1)–N(3) = 81.63(6), N(1)–Co(1)–N(2) = 81.61(6), N(4)–Co(1)–N(2) = 179.20(7), N(3)–Co(1)–N(2) = 99.15(6), Cl(1)–Co(1)–Cl(2) = 179.052(19), O(1)–H(20)–O(2) = 169.29(15). r.t. = room temperature.

both anodic and cathodic peaks of the Co(II)/Co(I) system are directly proportional to the scan rate (Supplementary Fig. S3), which confirms the immobilization of the cobalt complexes on the electrode surface. Surface catalyst concentrations as high as $4.5\ (\pm 0.2) \times 10^{-9}$ mol cm^{-2} could be estimated from the
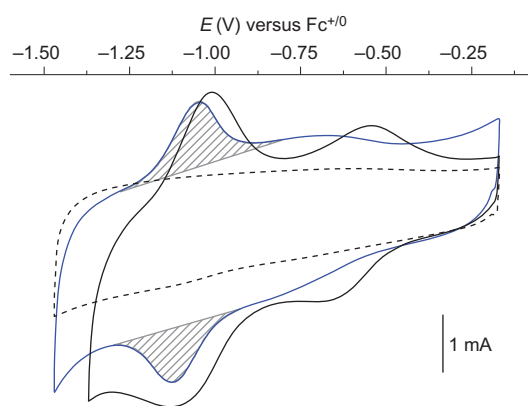
Figure 2 | Electrochemical characterization. Cyclic voltammogram (black line) of **3** in acetonitrile (0.1 M n-Bu$_4$NBF$_4$) recorded on a GDL/MWCNT electrode and the cyclic voltammogram (blue line) recorded on GDL/MWCNT/Co functionalized electrode material in acetonitrile (0.1 M Et$_4$NCl), compared with the blank GDL/MWCNT electrode (dotted line). All data have been obtained at 100 mV·s^{-1}. Integration of the electrochemical wave (shaded area) allows an estimation of the electroactive Co species on the functionalized electrode.

integration of this mono-electronic wave (Fig. 2). The indicated error accounts for the dispersion of results measured at different scan rates and on five distinct samples. X-ray photoelectron spectroscopy (XPS) analysis (Fig. 3 and Supplementary Fig. S4) confirmed the presence of the diimine–dioxime cobalt complex at the surface of the electrode. By comparison to the spectrum of amino-decorated MWCNTs (red line in Fig. 3; nitrogen is not detected in the black line of pristine MWCNTs), the XPS analysis of the CNT/Co sample (blue line in Fig. 3; see Supplementary Table S1) shows an increase in the nitrogen peak intensity as well as two sharp peaks in the Co region with binding energies of

781.7 eV and 796.6 eV, which correspond to the $2p_{3/2}$ and $2p_{1/2}$ levels in a 2:1 ratio. The difference of 14.9 eV between the peaks and the absence of a shake-up satellite on the Co $2p$ core level signals are clear evidence of the presence of the Co(III) ion. Considering that the peak obtained at 284.4 eV in the decomposition of the C 1s energy level signal with three Gaussian–Lorentzian curves[32] corresponds mainly to the electrons collected from the sp^2 carbons of the CNTs, calculation of the intensity ratio Co $2p_{3/2}$/C1 $2p_{3/2}$ and $2p_{1/2}$ allows us to estimate about one cobalt atom for 310 carbons (Supplementary Fig. S5).

The scanning electron micrograph (SEM) of the CNT/Co electrode (Supplementary Fig. S6) shows the homogeneous deposit of CNTs and confirms the absence of large conglomerates or nanoparticles after derivatization.

Catalytic hydrogen evolution. So far, catalytic H$_2$ evolution mediated by diimine–dioxime cobalt complexes has been observed only in non-aqueous solvents[28,33]. In the following we show that the new molecular-based CNT/Co material is catalytically competent for H$_2$ evolution from fully aqueous electrolytes at a mild pH. We first ran a linear sweep voltammetry experiment recorded on a CNT/Co electrode (Fig. 4a, blue solid line) in acetate buffer solution (0.1 M, pH 4.5). During the experiment N$_2$ was bubbled continuously through the electrolyte at a constant flow and the output gas was analysed every two minutes by gas chromatography (see the Supplementary Information). H$_2$ could be detected by gas chromatography from −0.35 V versus a reversible hydrogen electrode (RHE; 350 mV onset overpotential, blue dotted line), which compares well with the overpotential requirement (290 mV) determined for [Co(DO)(DOH)pnBr$_2$] in CH$_3$CN (ref. 16). An overpotential value of 590 mV was required to reach a current density of 1 mA cm^{-2}. By comparison, unfunctionalized GDL/MWCNT electrodes (black lines in Fig. 4a) display a much lower catalytic H$_2$-evolution activity. Tafel analysis (Supplementary Fig. S10) gave a Tafel slope of 160 mV per decade and an exchange current
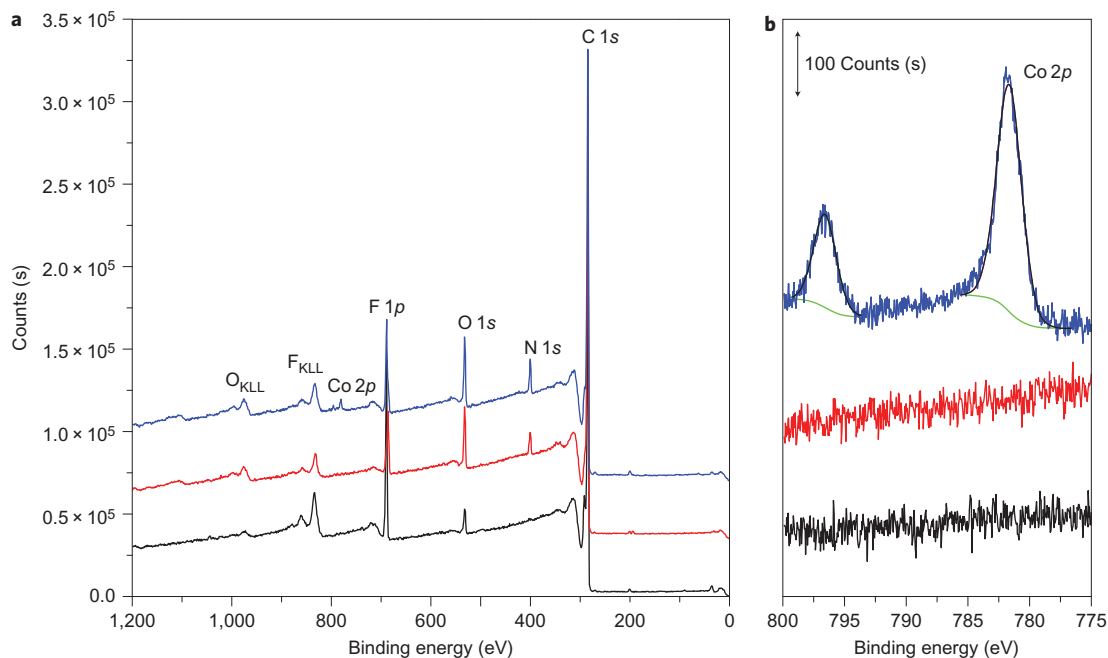

Figure 3 | XPS analysis. a,b, Survey (**a**) and Co 2p core level (**b**) spectra of pristine MWCNTs (black), amino-decorated MWCNTs (red) and CNT/Co material (blue) supported on fluorinated GDL substrates. The oxygen and fluorine present in the samples arose from defects (alcohol or carboxylic acid functions) on the MWCNTs and from the fluorinated GDL membrane support, respectively. A careful analysis of the survey spectrum of pristine MWCNTs clearly shows the absence of metallic contaminants. The CNT/Co material was prepared in the absence of Nafion to minimize the fluorine signal. KLL indicates Auger transitions.
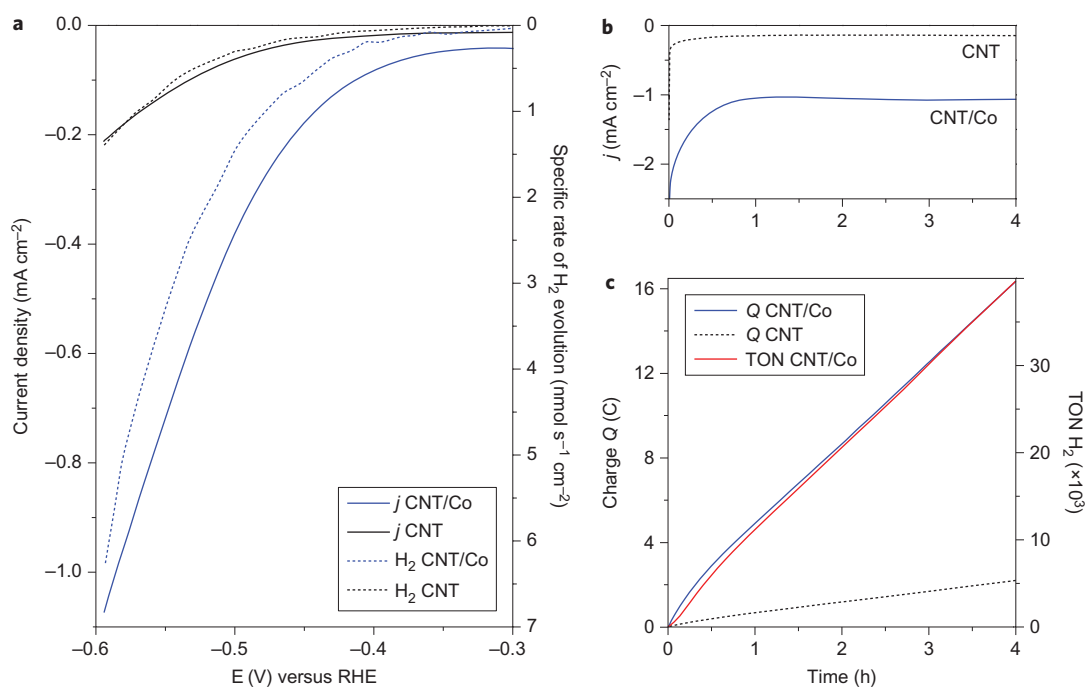
Figure 4 | Electrocatalytic hydrogen evolution. a, Linear sweep voltammetry (solid lines) recorded on a GDL/MWCNT/Co electrode (blue line) compared with that of an unfunctionalized GDL/MWCNT electrode (black line) in acetate buffer (0.1 M, pH 4.5) at low scan rates (0.1 mV s^{-1}) with simultaneous monitoring of H$_2$ evolution (dotted lines; N$_2$ was bubbled continuously through the electrolyte at a constant flow (5 ml·min^{-1}) during the experiment and the concentration of H$_2$ in the output gas was determined every two minutes by gas chromatography; Faradaic yield, 100%). The use of an acetate buffer/NaCl solution (0.1 M, pH 4.5) did not result in increased activity. **b,** Evolution of the current density during an electrolysis experiment run on a GDL/MWCNT/Co electrode (solid blue line) compared with that of a blank GDL/MWCNT electrode (black dotted line) at −0.59 V versus RHE in acetate buffer (0.1 M, pH 4.5). **c,** Charge passed during the same experiment (solid blue line) and the corresponding turnover numbers (TON, solid red line) for electrocatalytic H$_2$ production.

density of $10^{-6.5}$ A cm$^{-2}_{\text{geometric}}$. This value is comparable to that reported for electrodeposited MoS$_2$ catalysts ($10^{-6.5}$ A cm$^{-2}_{\text{geometric}}$) (ref. 34). For comparison, NiMo-based materials exhibit current densities between 10^{-6} and $10^{-3.5}$ A cm$^{-2}_{\text{geometric}}$ (refs 35,36).

Material stability and mechanistic insights. For the catalytic stability assessment, the electrode was then equilibrated at a constant potential of −0.59 V versus RHE in acetate buffer. As shown in Fig. 4b, the current density stabilized after about one hour at a constant value of approximately 1 mA cm^{-2}. Considering that two electrons are required for the formation of a H$_2$ molecule and using the determined surface concentration of the catalyst (4.5 ($\pm$0.2) $\times 10^{-9}$ mol cm^{-2}), we calculated a turnover frequency per grafted Co catalyst of ~8,000 ($\pm$5%) h^{-1}. Over a four hour experiment and after subtraction of the control experiment, a turnover number of 33,000 ($\pm$5%) could be determined with a near-quantitative Faradaic yield (0.97$\pm$0.05). During a longer experiment, 55,000 ($\pm$5%) turnovers were performed in seven hours with a similar Faradaic efficiency. These values compare well with those obtained when nickel-based H$_2$-evolving catalysts were grafted on MWCNTs through similar methods[18,19].

Remarkably, in comparison with previous solution studies for [Co(DO)(DOH)pnBr$_2$] that showed significant degradation after 50 turnovers[28], the stability of the present molecular catalyst was enhanced by several orders of magnitude after immobilization on the electrode. Although as yet no detailed 'post-mortem' analysis is reported for cobaloxime or diimine–dioxime catalysts, a recent report on the related diimine–dipyridine metal complexes[37] shows that reductive processes at the metal site may generate transient carbon-based α-imino radical species that can undergo reductive homocoupling to yield dimer complexes with new metal coordination spheres, probably not suitable for catalysis. Once grafted onto electrode materials, the molecular complexes are isolated and

may not be able to react in such a bimolecular manner. Additionally, the supply of electrons from CNTs to the catalyst is optimized in the CNT/Co material, which should significantly limit the lifetime of reduced intermediates along the catalytic cycle and consequently avoid degradative side reactions. We believe that these are the two main crucial reasons for the enhanced stability observed with the surface attachment as compared with homogeneous studies. Grafting thus provides an avenue for achieving the full benefit from the redox non-innocence of coordinated ligands for the design of active molecular electrocatalysts.

Another exciting observation was that the surface of the electrode after an electrolysis experiment did not show any alteration of the grafted complex. Indeed, XPS measurements revealed the same surface composition (Supplementary Fig. S8). In the Co region, the two broad sets of signals that correspond to the 2$p_{3/2}$ and 2$p_{1/2}$ core levels are still observed. The absence of any peak below 780.9 eV excludes the presence of cobalt oxide or metallic cobalt on the surface. SEM images (Supplementary Fig. S6) are indistinguishable from those recorded immediately after derivatization. Cyclic voltammograms recorded in CH$_3$CN (Supplementary Fig. S9) show that the signal of the Co(II)/Co(I) couple of the grafted complex remains unchanged, both in position and intensity. Thus we can rule out the formation of reactive metallic or metal-oxide particles and assign the catalytic activity exclusively to the intact grafted molecular complex. In addition, no H$_2$ evolution activity could be detected when the CNT/Co material was assayed in aqueous phosphate buffer (pH 7, Supplementary Fig. S7), probably because the grafted molecular catalysts require a more acidic environment for cycling. This observation clearly excludes any reductive transformation of the grafted molecular complex into the nanoparticulate H$_2$–CoCat material that we reported recently and that would spontaneously form under these conditions if the molecular complex was free in solution[38]. This is a quite unique

situation compared to the frequent reports that such particles, derived from the decomposition of molecular catalysts in solution[38–42] or heterogeneized[43,44], are at least partly[45] responsible for catalysis.

Thus, this is the first time that a molecular and mononuclear cobalt complex grafted at the surface of an electrode was found to be catalytically active. This allows us to derive some conclusions regarding the mechanism at work during catalysis, an issue discussed thoroughly over the past five years in the case of cobaloxime catalysts[5,6]. Two distinct mechanisms were considered for catalysts in solution, and both involve a metal-hydride species as the key intermediate: (1) in the homolytic mechanism, two metal–hydride complexes evolve H_2 through a reductive elimination reaction; (2) in the alternative heterolytic pathway, the intermediate metal–hydride species decompose by proton attack and evolve H_2 via an intermediate dihydrogen complex. At the surface of an electrode two distinct immobilized centres are unlikely to react together, which rules out the homolytic mechanism. Further mechanistic studies are still needed to assign definitively the oxidation state of the active species during catalysis, in line with recent theoretical studies on cobaloxime catalysts that favour Co(II)–H over Co(III)–H species in the heterolytic pathway[46,47].

Conclusions

Tetraimine cobalt complexes are among the most efficient molecular catalysts for H_2 evolution. We demonstrate here, for the first time, the successful integration of a diimine–dioxime cobalt catalyst coupled to CNTs to give a very active electrocatalytic cathode material for H_2 generation from fully aqueous solutions, from an overpotential of 350 mV. Around 55,000 turnovers were obtained during seven hours of electrolysis in acetate buffer at a potential of −0.59 V versus RHE. This material is remarkably stable, which allows extensive cycling with no alteration of the grafted molecular complex. Clearly, this indicates that grafting provides a largely increased stability to these cobalt catalysts and thus paves the way towards their development in technological devices.

Methods

Solvents and starting materials were purchased from Sigma-Aldrich and used without further purification, unless otherwise stated. When necessary, solvents were distilled under argon: diethylether was distilled by refluxing over sodium/benzophenone; dry acetonitrile and dichloromethane were obtained by distillation on CaH$_2$. The (4-aminoethyl)benzenediazonium tetrafluoroborate salt was prepared as described previously[48]. All reactions in solution were performed routinely under an inert atmosphere of argon using conventional vacuum-line and glasswork techniques. However, the metal complexes were handled in air in the solid state. Commercial grade NC3100 MWCNTs were obtained from Nanocyl (purity >95% in carbon) and used as received. Thermogravimetric and XPS analyses of MWCNT batches showed the absence of amorphous carbon and the high purity of the MWCNTs, with only 3.4% of inorganic materials analysed as SiO$_2$. No metallic impurities were detected by XPS (these data were reported recently by Morozan et al.[49]). The GDL substrate was purchased from GORE Fuel Cell Technologies (CARBEL CL-P-02360).

Characterization methods and equipment are described in the Supplementary Information.

Preparation of GDL/MWCNT electrodes. In a typical experiment, a suspension of MWCNTs (2 mg) and Nafion (200 µl of a 5% solution in alcohol/water) in ethanol (200 ml) was sonicated until solubilization was complete (ten minutes). The MWCNT solution was deposited by slow filtration onto a GDL support (surface 10 cm^2). The resulting material was air dried for ten minutes and then heated for 30 min in an oven at 80 °C. The estimated MWCNT charge was 0.2 mg·cm$^{−2}$.

Amine electrofunctionalization of the GDL/MWCNT electrodes. The method is based on a literature procedure[18]. The GDL/MWCNT material was employed as a working electrode in an electrochemical cell in the presence of (4-aminoethyl)benzene diazonium tetrafluoroborate (16 mg, 0.07 mmol) in a tetrabutylammonium tetrafluoroborate electrolyte solution (0.1 M) in acetonitrile (50 ml). Electrografting was performed through reduction of the diazonium salt by cyclic voltammetry, recording three cycles at 20 mV·s$^{−1}$ between 0.0 V and −1.5 V versus Fc$^{+/0}$. The amine-functionalized electrode was washed three times by dipping in acetonitrile (ten minutes) and dried under a flow of nitrogen. A control sample was cut and used to measure the blank signal.

Preparation of 2. To a solution of ligand **1** (197 mg, 0.70 mmol, see the Supplementary Information) in acetone (20 ml) was added a solution of CoCl$_2$·6H$_2$O (166 mg, 0.70 mmol) in acetone (10 ml). The mixture was stirred for 2 h under a continuous bubbling of air. The resulting green precipitate was filtered off, dissolved in CH$_3$CN, filtered and the solvent evaporated. The same operation was carried out with CH$_2$Cl$_2$ to yield a green powder (227 mg, 79% yield). ^{1}H NMR (300 MHz, acetone-d_6): δ ppm 19.40 (s, 1H, OHO), 4.62–4.53 (m, 3H, CH$_2$, CHN$_3$), 3.88 (t, J = 13.2 Hz, 2H, CH$_2$), 2.77 (d, J = 1.7 Hz, 6H, CH$_3$), 2.55 (s, 6H, CH$_3$). ^{13}C NMR (75 MHz, DMSO-d_6): δ ppm 176.9, 155.9, 58.6, 54.0, 18.2, 13.7. MS (ESI$^−$): m/z 407.8 [M–H]$^−$. Elemental analysis calculated (%) for C$_{11}$H$_{18}$Cl$_2$CoN$_7$O$_2$·0.4C$_3$H$_6$O: C, 33.70; H, 4.72; N, 22.72; found: C, 33.34; H, 4.60; N 22.35.

Preparation of 3. A solution of **2** (200 mg, 0.48 mmol) and N-phthalimidyl-2-(cyclooct-2-yn-1-yloxy)acetate **V** (165 mg, 1 equiv., see the Supplementary Information) in distilled CH$_3$CN (15 ml) was stirred at room temperature for 24 h. After concentration under vacuum, the reaction mixture was purified on a Sephadex LH20 column (eluent: acetone/CH$_2$Cl$_2$, 1/1). The first fractions were evaporated and dried under vacuum to give a green powder (279 mg, 75 %). ^{1}H NMR (300 MHz, acetone-d_6): δ ppm 19.45 (s, 1H, OH), 7.98 (s, 4H, Ph), 5.80–5.52 (m, 1H, CH–O), 5.06 (ddd, J = 12.0, 7.7, 3.5 Hz, 1H, CH–N), 4.77 (dd, J = 27.3, 16.8 Hz, 2H, CH$_2$–N), 4.66 (s, 2H, CH$_2$–O), 4.75–4.39 (m, 2H, CH$_2$–N), 3.06 (dtd, J = 21.8, 14.9, 7.0 Hz, 2H, CH$_2$-oct), 2.68 (dd, J = 31.3, 1.2 Hz, 6H, CH$_3$), 2.59 (d, J = 11.8 Hz, 6H, CH$_3$), 2.30–2.19 (m, 1H, CH$_2$-oct), 1.99–1.91 (m, 1H, CH$_2$-oct), 1.87–1.13 (m, 6H, CH$_2$-oct). MS (ESI$^+$): m/z 701.3 [M–Cl]$^−$. Elemental analysis calculated (%) for C$_{29}$H$_{35}$Cl$_2$CoN$_8$O$_7$·0.5CH$_2$Cl$_2$: C, 45.85; H, 4.62; N, 14.26; found: C, 46.08; H, 5.01; N, 13.89.

Covalent grafting of cobalt catalyst 3 on the amino electrofunctionalized GDL/MWCNT electrode. The amine electrofunctionalized GDL/MWCNT material was dipped in a 1 mM solution of cobalt catalyst **3** (3.5 mg) in distilled CH$_2$Cl$_2$ (5 ml) in the presence of 2,6-dimethylpyridine (5 µl, 8 equiv.) and agitated for 24 h. The resulting cobalt-functionalized electrode was then removed from the solution, washed by dipping in CH$_2$Cl$_2$ and then CH$_3$CN (ten minutes each) and dried under a flow of nitrogen.

For electrochemical studies, the functionalized electrode material was cut into several pieces and the active surface was delimited using solvent-resistant epoxy glue. The electrical contacts were made using conductive silver-based glue and a metallic wire. An identical procedure was used to prepare the control samples.

References

1. Armaroli, N. & Balzani, V. The future of energy supply: challenges and opportunities. *Angew. Chem. Int. Ed.* **46,** 52–66 (2007).
2. Armaroli, N. & Balzani, V. The hydrogen issue. *ChemSusChem* **4,** 21–36 (2011).
3. Crabtree, G. W. & Dresselhaus, M. S. The hydrogen fuel alternative. *Mater. Res. Soc. Bull.* **33,** 421–428 (2008).
4. Gordon, R. B., Bertram, M. & Graedel, T. E. Metal stocks and sustainability. *Proc. Natl Acad. Sci. USA* **103,** 1209–1214 (2006).
5. Artero, V., Chavarot-Kerlidou, M. & Fontecave, M. Splitting water with cobalt. *Angew. Chem. Int. Ed.* **50,** 7238–7266 (2011).
6. Dempsey, J. L., Brunschwig, B. S., Winkler, J. R. & Gray, H. B. Hydrogen evolution catalyzed by cobaloximes. *Acc. Chem. Res.* **42,** 1995–2004 (2009).
7. Kanan, M. W. & Nocera, D. G. *In situ* formation of an oxygen-evolving catalyst in neutral water containing phosphate and Co^{2+}. *Science* **321,** 1072–1075 (2008).
8. Jiao, F. & Frei, H. Nanostructured cobalt oxide clusters in mesoporous silica as efficient oxygen-evolving catalysts. *Angew. Chem. Int. Ed.* **48,** 1841–1844 (2009).
9. Yin, Q. S. *et al.* A fast soluble carbon-free molecular water oxidation catalyst based on abundant metals. *Science* **328,** 342–345 (2010).
10. Risch, M. *et al.* Cobalt-oxo core of a water-oxidizing catalyst film. *J. Am. Chem. Soc.* **131,** 6936–6937 (2009).
11. Dau, H. *et al.* The mechanism of water oxidation: from electrolysis via homogeneous to biological catalysis. *ChemCatChem* **2,** 724–761 (2010).
12. Baffert, C., Artero, V. & Fontecave, M. Cobaloximes as functional models for hydrogenases. 2. Proton electroreduction catalyzed by difluoroboryl bis(dimethyl glyoximato)cobalt(II) complexes in organic media. *Inorg. Chem.* **46,** 1817–1824 (2007).
13. Hu, X. L., Cossairt, B. M., Brunschwig, B. S., Lewis, N. S. & Peters, J. C. Electrocatalytic hydrogen evolution by cobalt difluoroboryl–diglyoximate complexes. *Chem. Commun.* 4723–4725 (2005).
14. Razavet, M., Artero, V. & Fontecave, M. Proton electroreduction catalyzed by cobaloximes: functional models for hydrogenases. *Inorg. Chem.* **44,** 4786–4795 (2005).
15. Hu, X., Brunschwig, B. S. & Peters, J. C. Electrocatalytic hydrogen evolution at low overpotentials by cobalt macrocyclic glyoxime and tetraimine complexes. *J. Am. Chem. Soc.* **129,** 8988–8998 (2007).

5

16. Fourmond, V., Jacques, P. A., Fontecave, M. & Artero, V. H$_2$ evolution and molecular electrocatalysts: determination of overpotentials and effect of homoconjugation. *Inorg. Chem.* **49**, 10338–10347 (2010).

17. Helm, M. L., Stewart, M. P., Bullock, R. M., DuBois, M. R. & DuBois, D. L. A synthetic nickel electrocatalyst with a turnover frequency above 100,000 s^{-1} for H$_2$ production. *Science* **333**, 863–866 (2011).

18. Le Goff, A. *et al.* From hydrogenases to noble metal-free catalytic nanomaterials for H$_2$ production and uptake. *Science* **326**, 1384–1387 (2009).

19. Tran, P. D. *et al.* Noncovalent modification of carbon nanotubes with pyrene-functionalized nickel complexes: carbon monoxide tolerant catalysts for hydrogen evolution and uptake. *Angew. Chem. Int. Ed.* **50**, 1371–1374 (2011).

20. Toma, F. M. *et al.* Efficient water oxidation at carbon nanotube–polyoxometalate electrocatalytic interfaces. *Nature Chem.* **2**, 826–831 (2010).

21. Li, F. *et al.* Highly efficient oxidation of water by a molecular catalyst immobilized on carbon nanotubes. *Angew. Chem. Int. Ed.* **50**, 12276–12279 (2011).

22. DeKrafft, K. E. *et al.* Electrochemical water oxidation with carbon-grafted iridium complexes. *ACS Appl. Mater. Interfaces* **4**, 608–613 (2012).

23. Le Goff, A. *et al.* Facile and tunable functionalization of carbon nanotube electrodes with ferrocene by covalent coupling and pi-stacking interactions and their relevance to glucose bio-sensing. *J. Electroanal. Chem.* **641**, 57–63 (2010).

24. Tasis, D., Tagmatarchis, N., Bianco, A. & Prato, M. Chemistry of carbon nanotubes. *Chem. Rev.* **106**, 1105–1136 (2006).

25. Sgobba, V. & Guldi, D. M. Carbon nanotubes – electronic/electrochemical properties and application for nanoelectronics and photonics. *Chem. Soc. Rev.* **38**, 165–184 (2009).

26. Clave, G. & Campidelli, S. Efficient covalent functionalisation of carbon nanotubes: the use of 'click chemistry'. *Chem. Sci.* **2**, 1887–1896 (2011).

27. Pinson, J. & Podvorica, F. Attachment of organic layers to conductive or semiconductive surfaces by reduction of diazonium salts. *Chem. Soc. Rev.* **34**, 429–439 (2005).

28. Jacques, P-A., Artero, V., Pécaut, J. & Fontecave, M. Cobalt and nickel diimine–dioxime complexes as molecular electrocatalysts for hydrogen evolution with low overvoltages. *Proc. Natl Acad. Sci. USA* **106**, 20627–20632 (2009).

29. Kolb, H. C., Finn, M. G. & Sharpless, K. B. Click chemistry: diverse chemical function from a few good reactions. *Angew. Chem. Int. Ed.* **40**, 2004–2021 (2001).

30. Sletten, E. M. & Bertozzi, C. R. From mechanism to mouse: a tale of two bioorthogonal reactions. *Acc. Chem. Res.* **44**, 666–676 (2011).

31. Seeber, R., Parker, W. O., Marzilli, P. A. & Marzilli, L. G. Electrochemical synthesis of Costa-type cobalt complexes. *Organometallics* **8**, 2377–2381 (1989).

32. Palacin, S. *et al.* Efficient functionalization of carbon nanotubes with porphyrin dendrons via click chemistry. *J. Am. Chem. Soc.* **131**, 15394–15402 (2009).

33. Berben, L. A. & Peters, J. C. Hydrogen evolution by cobalt tetraimine catalysts adsorbed on electrode surfaces. *Chem. Commun.* **46**, 398–400 (2010).

34. Jaramillo, T. F. *et al.* Identification of active edge sites for electrochemical H$_2$ evolution from MoS$_2$ nanocatalysts. *Science* **317**, 100–102 (2007).

35. McKone, J. R. *et al.* Evaluation of Pt, Ni, and Ni–Mo electrocatalysts for hydrogen evolution on crystalline Si electrodes. *Energy Environ. Sci.* **4**, 3573–3583 (2011).

36. Chen, W-F. *et al.* Hydrogen-evolution catalysts based on non-noble metal nickel–molybdenum nitride nanosheets. *Angew. Chem. Int. Ed.*, **51**, 6131–6135 (2012).

37. Hulley, E. B., Wolczanski, P. T. & Lobkovsky, E. B. Carbon–carbon bond formation from azaallyl and imine couplings about metal–metal bonds. *J. Am. Chem. Soc.* **133**, 18058–18061 (2011).

38. Cobo, S. *et al.* A Janus cobalt-based catalytic material for electro-splitting of water. *Nature Mater.* **11**, 802–807 (2012).

39. Blakemore, J. D. *et al.* Anodic deposition of a robust iridium-based water-oxidation catalyst from organometallic precursors. *Chem. Sci.* **2**, 94–98 (2011).

40. Widegren, J. A. & Finke, R. G. A review of the problem of distinguishing true homogeneous catalysis from soluble or other metal–particle heterogeneous catalysis under reducing conditions. *J. Mol. Catal. A* **198**, 317–341 (2003).

41. Stracke, J. J. & Finke, R. G. Electrocatalytic water oxidation beginning with the cobalt polyoxometalate [Co$_4$(H$_2$O)$_2$(PW$_9$O$_{34}$)$_2$]$^{10-}$: Identification of heterogeneous CoO$_x$ as the dominant catalyst. *J. Am. Chem. Soc.* **133**, 14872–14875 (2011).

42. Anxolabehere-Mallart, E. *et al.* Boron-capped tris(glyoximato) cobalt clathrochelate as a precursor for the electrodeposition of nanoparticles catalyzing H$_2$ evolution in water. *J. Am. Chem. Soc.* **134**, 6104–6107 (2012).

43. Hocking, R. K. *et al.* Water-oxidation catalysis by manganese in a geochemical-like cycle. *Nature Chem.* **3**, 461–466 (2011).

44. Wiechen, M., Berends, H. M. & Kurz, P. Water oxidation catalysed by manganese compounds: from complexes to 'biomimetic rocks'. *Dalton Trans.* **41**, 21–31 (2012).

45. Schley, N. D. *et al.* Distinguishing homogeneous from heterogeneous catalysis in electrode-driven water oxidation with molecular iridium complexes. *J. Am. Chem. Soc.* **133**, 10473–10481 (2011).

46. Muckerman, J. T. & Fujita, E. Theoretical studies of the mechanism of catalytic hydrogen production by a cobaloxime. *Chem. Commun.* **47**, 12456–12458 (2011).

47. Solis, B. H. & Hammes-Schiffer, S. Theoretical analysis of mechanistic pathways for hydrogen evolution catalyzed by cobaloximes. *Inorg. Chem.* **50**, 11252–11262 (2011).

48. Griveau, S., Mercier, D., Vautrin-Ul, C. & Chaussé, A. Electrochemical grafting by reduction of 4-amino-ethylbenzenediazonium salt: application to the immobilization of (bio)molecules. *Electrochem. Commun.* **9**, 2768–2773 (2007).

49. Morozan, A. *et al.* Metal-free nitrogen-containing carbon nanotubes prepared from triazole and tetrazole derivatives show high electrocatalytic activity towards the oxygen reduction reaction in alkaline media. *ChemSusChem* **5**, 647–651 (2012).

Author contributions

V.A., B.J., S.P. and M.F. designed the research, E.S.A., P-A.J., P.D.T., A.L., M.C-K., M.M. and V.A. performed the research, J.P. performed the X-ray crystallographic studies and V.A. and E.S.A. co-wrote the paper.

Additional information

Supplementary information and chemical compound information are available in the online version of the paper. Reprints and permission information is available online at http://www.nature.com/reprints. Correspondence and requests for materials should be addressed to V.A.

Competing financial interests

Patent applications (EP-08 290 988.8 and E.N.10 53019) have been filed for the preparation of azide-appended diimine–dioxime complexes such as **2** and their grafting onto electrode materials.